Suenson, E., & Thorsen, S. (1981) *Biochem. J. 197*, 619–628.
Sugiyama, N., Sasaki, T., Iwamoto, M., & Abiko, Y. (1988) *Biochim. Biophys. Acta 952*, 1–7.
Thewes, T., Ramesh, V., Simplaceanu, E., & Llinás, M. (1987) *Biochim. Biophys. Acta 912*, 254–269.
Thewes, T., Constantine, K., Byeon, I., & Llinás, M. (1990) *J. Biol. Chem. 265*, 3906–3915.
Thorsen, S. (1975) *Biochim. Biophys. Acta 393*, 55–65.
Trexler, M., Vâli, Z., & Patthy, L. (1982) *J. Biol. Chem. 257*, 7401–7406.
Tulinsky, A. (1991) in Proceedings of the XIII International Society of Thrombosis and Haemostasis Congress, Amsterdam, *Thrombosis Haemostasis 66*, 16–31.
Tulinsky, A., Park, C. H., Mao, B., & Llinás, M. (1988) *Proteins: Struct., Funct., Genet. 3*, 85–96.
Vâli, Z., & Patthy, L. (1982) *J. Biol. Chem. 257*, 2104–2110.
Vâradi, A., & Patthy, L. (1981) *Biochem. Biophys. Res. Commun. 103*, 97–102.
Wider, G., Macura, S., Kumar, A., Ernst, R., & Wüthrich, K. (1984) *J. Magn. Reson. 56*, 207–234.
Wiman, B., Boman, L., & Collen, D. (1978) *Eur. J. Biochem. 87*, 143–146.
Wiman, B., Lijnen, H. R., & Collen, D. (1979) *Biochim. Biophys. Acta 579*, 142–154.
Winn, E., Hu, S. P., Hochschwender, S., & Laursen, R. (1980) *Eur. J. Biochem. 104*, 579–586.

Investigation of the Functional Role of Tryptophan-22 in *Escherichia coli* Dihydrofolate Reductase by Site-Directed Mutagenesis[†,‡]

Mark S. Warren,[§] Katherine A. Brown,[§] Martin F. Farnum,[§] Elizabeth E. Howell,[∥] and Joseph Kraut*[,§]

Department of Chemistry, University of California, San Diego, La Jolla, California 92093, and Department of Biochemistry, Walters Life Science Building, University of Tennessee, Knoxville, Tennessee 37996

Received June 4, 1991; Revised Manuscript Received August 22, 1991

ABSTRACT: We have applied site-directed mutagenesis methods to change the conserved tryptophan-22 in the substrate binding site of *Escherichia coli* dihydrofolate reductase to phenylalanine (W22F) and histidine (W22H). The crystal structure of the W22F mutant in a binary complex with the inhibitor methotrexate has been refined at 1.9-Å resolution. The W22F difference Fourier map and least-squares refinement show that structural effects of the mutation are confined to the immediate vicinity of position 22 and include an unanticipated 0.4-Å movement of the methionine-20 side chain. A conserved bound water-403, suspected to play a role in the protonation of substrate DHF, has *not* been displaced by the mutation despite the loss of a hydrogen bond with tryptophan-22. Steady-state kinetics, stopped-flow kinetics, and primary isotope effects indicate that both mutations increase the rate of product tetrahydrofolate release, the rate-limiting step in the case of the wild-type enzyme, while slowing the rate of hydride transfer to the point where it now becomes at least partially rate determining. Steady-state kinetics show that below pH 6.8, k_{cat} is elevated by up to 5-fold in the W22F mutant as compared with the wild-type enzyme, although $k_{cat}/K_{m(dihydrofolate)}$ is lower throughout the observed pH range. For the W22H mutant, both k_{cat} and $k_{cat}/K_{m(dihydrofolate)}$ are substantially lower than the corresponding wild-type values. While both mutations weaken dihydrofolate binding, cofactor NADPH binding is not significantly altered. Fitting of the kinetic pH profiles to a general protonation scheme suggests that the proton affinity of dihydrofolate may be enhanced upon binding to the enzyme. We suggest that the function of tryptophan-22 may be to properly position the side chain of methionine-20 with respect to N5 of the substrate dihydrofolate.

Dihydrofolate reductase (DHFR,[1] EC 1.5.1.3) catalyzes the NADPH-dependent reduction of 7,8-dihydrofolate (DHF) to 5,6,7,8-tetrahydrofolate (THF). This activity is required to maintain intracellular pools of THF and its derivatives, which are essential cofactors in the transfer of one-carbon units in the biosynthesis of thymidylate, purine nucleotides, and some amino acids. Inhibition of DHFR activity by folate analogues and related compounds is important in the treatment of several diseases. Examples of these clinically useful compounds include the anticancer drug methotrexate (MTX), the antibacterial agent trimethoprim, and the antimalarial drug pyrimethamine.

[†] Based on the Ph.D. dissertation of M.S.W., supported by NIH Grants GM10928 to J.K. and GM35308 to E.E.H.

[‡] The coordinates for the recombinant wild-type *E. coli* dihydrofolate reductase and the W22F mutant have been submitted to the Brookhaven Protein Data Bank and have been assigned entry numbers 1DRC and 2DRC, respectively.

* Author to whom correspondence should be addressed.
[§] University of California.
[∥] University of Tennessee.

[1] Abbreviations: DHFR, dihydrofolate reductase; DHF, dihydrofolate; THF, tetrahydrofolate; MTX, methotrexate; NADPH, nicotinamide adenine dinucleotide phosphate (reduced form); wt, wild type; W22F, Trp-22 → Phe mutant dihydrofolate reductase; W22H, Trp-22 → His mutant dihydrofolate reductase; lc:W21L, Trp-21 → Leu mutant *Lactobacillus casei* dihydrofolate reductase; m:W24R, Trp-24 → Arg mutant mouse dihydrofolate reductase; h:W24F, Trp-24 → Phe mutant human dihydrofolate reductase; *E. coli*, *Escherichia coli*; *L. casei*, *Lactobacillus casei*.

$$R_{sym} = \sum_{hkl} \frac{\sum_i |I_i - \bar{I}|}{\sum_i I_i}$$

$$R\text{-factor} = \frac{\sum_{hkl} |F_o - F_c|}{\sum_{hkl} F_o}$$

0006-2960/91/0430-11092$02.50/0

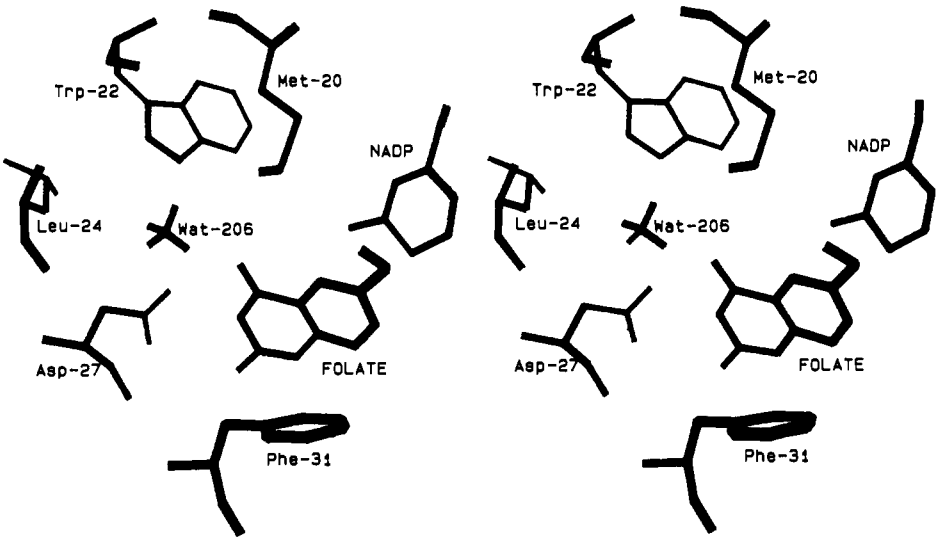

FIGURE 1: Stereopair diagram of the catalytic site in wt DHFR, from the ternary DHFR·folate·NADP$^+$ structure (Bystroff et al., 1990). The pteridine ring of folate and the nicotinamide ring of NADP$^+$ are shown.

Crystal structures of DHFR from *Escherichia coli*, as well as DHFRs from other bacterial and vertebrate sources, have been solved and refined to high resolution in complexes with various ligands (Matthews et al., 1977, 1978, 1979, 1985a,b; Bolin et al., 1982; Filman et al., 1982; Volz et al., 1982; Stammers et al., 1987; Oefner et al., 1988; Bystroff et al., 1990; Davies et al., 1990; Bystroff & Kraut, 1991). These structures have paved the way for experiments which, through the use of site-directed mutagenesis, have attempted to define the precise role of specific amino acids in ligand binding and catalysis (Villafranca et al., 1983; Howell et al., 1986, 1987; Chen et al., 1987; Taira et al., 1988; Benkovic et al., 1988; Thillet et al., 1988; Murphy & Benkovic, 1989; Fierke & Benkovic, 1989; Adams et al., 1989; Schweitzer et al., 1989; Prendergast et al., 1989; Tsay et al., 1990).

It is generally believed that the catalytic mechanism of DHFR requires DHF to be protonated at N5 of the dihydropterin ring in order to facilitate hydride transfer from C4 of the nicotinamide ring of NADPH to C6 of DHF (Stone & Morrison, 1988; Morrison & Stone, 1988). Previous site-directed mutagenesis experiments have shown a conserved acidic residue, Asp-27, to be crucial in the protonation of the substrate DHF. Mutants in which Asp-27 was replaced by asparagine or serine could only function effectively by binding DHF which was pre-protonated in solution (Villafranca et al., 1983; Howell et al., 1986). Since the pK for N5 of the pteridine ring of DHF is 2.59 (Maharaj et al., 1990), these mutant enzymes have activities at neutral pH which are considerably lower than k_{cat} of the wild-type (wt) enzyme, since at pH 7 very little of the DHF is protonated in solution. However, at lower pH where more of the DHF is protonated in solution, the steady-state activities of these mutant enzymes increase to the point where k_{cat} of the Asp-27 → Ser mutant enzyme becomes comparable with that of the wt enzyme.

Although Asp-27 is required for the protonation of substrate, it is still unclear what the immediate source of the proton is or how it is transferred to N5 of DHF, as the carboxylic acid side chain of Asp-27 is about 6 Å away from the N5–C6 double bond of DHF, and N5 is buried in a hydrophobic environment composed of the side chains of Met-20 and Leu-28 (Bolin et al., 1982; Bystroff et al., 1990). Asp-27 may donate a proton itself, or it may catalyze proton donation by a water molecule while remaining protonated (Bystroff et al., 1990). This proton may be relayed to N5 via a fixed water molecule, water-403, that is present in every DHFR structure having a ligand in the pterin binding site.[2]

One of the residues that can form a hydrogen bond with water-403 is an invariant tryptophan, Trp-22. This active site tryptophan is evolutionarily conserved in every known chromosomally encoded DHFR sequence.[3] In the DHFR·MTX binary complex, Trp-22 makes hydrophobic interactions with Met-20 and Leu-24, as well as an indirect hydrogen bond with MTX through water-403. In the DHFR·folate·NADP$^+$ ternary complex, Trp-22 additionally makes van der Waals interactions with the nicotinamide of NADP$^+$ (see Figure 1). Trp-22 is also a key residue in the Met-20 loop of DHFR (composed of residues 9–23) which connects β-strand A to α-helix B. This loop serves as a "lid", closing over the bound ligands in the ternary complex (Bystroff et al., 1990). Because of its interactions with the relatively fixed Leu-24 of the α-β helix and the relatively floppy Met-20 of the Met-20 loop, Trp-22 is likely to be a key residue in the positioning of this loop in the ternary complex.

To investigate the roles of Trp-22 and (it was hoped, but see below) water-403, we have used site-directed mutagenesis to replace this tryptophan with phenylalanine (W22F) and with histidine (W22H). We have studied the effects of the Trp → Phe substitution on ligand binding and by X-ray crystallography, steady-state kinetics and pre-steady-state kinetics; the Trp → His substitution was similarly investigated except that we have been unable to obtain suitably diffracting crystals of the W22H mutant enzyme. We had expected that the W22F mutation would displace or eject water-403 and that loss of the hydrogen bond to Nϵ of Trp-22 and the proximity of a large hydrophobic phenylalanine side chain would force

[2] Water-403 is observed in complexes with various ligands and in DHFRs from various species, but it has been given different labels. For example, it is water-403 and water-603 in the two molecules of the asymmetric unit of the *E. coli* DHFR·MTX structure, water-206 in the ternary *E. coli* DHFR·folate·NADP$^+$ structure, water-253 in the *L. casei* DHFR·MTX·NADPH structure, and water-203 in the chicken liver DHFR·NADPH structure.

[3] Trp-22 is one of only 12 residues out of the 159 in *E. coli* DHFR that are conserved in all known eukaryotic, bacterial, and phage sequences (Lagosky et al., 1987; Blakley, 1984). These 12 residues are A7, G15, P21, W22, F31, T35, G43, T46, L54, R57, G95, and G96 (*E. coli* numbering system). The species compared are chicken, bovine, mouse, porcine, human, *Saccharomyces cerevisiae*, *L. casei*, *Streptococcus faecium*, *E. coli*, T4 phage, and Tn7 (type I). Although only 12 residues are absolutely conserved, many others are replaced by similar amino acids in the various species.

this water molecule out of its binding site. The crystallographic evidence shows that this did not occur. Nonetheless, these studies have shed some light on the the possible importance of water-403 and the function of Trp-22 in DHFR.

While this work was in progress, the same Trp → Phe mutant of recombinant human DHFR, h:W24F, was also characterized in detail (Huang et al., 1989; Beard et al., 1991). Additionally, two other mutations of this tryptophan in other species of DHFR were reported: to leucine in *L. casei*, lc: W21L (Andrews et al., 1989); and to arginine in mouse, m:W24R (Thillet et al., 1988). However, structures of these mutant DHFRs have not been reported.

All three of these mutations alter enzymic properties, although each does so to a different extent. The lc:W21L mutation significantly decreases the affinity for NADPH, while the others cause little alteration in NADPH binding. The h:W24F mutation increases k_{cat}, while the others, especially m:W24R, decrease k_{cat}. Stability was found to be substantially enhanced in m:W24R but decreased by 50% in h:W24F. Clearly, each mutation presents yet another piece that must be fitted into the enzyme structure–function puzzle.

Materials and Methods

The W22H and W22F mutations were constructed by oligonucleotide-directed site-specific mutagenesis of the cloned wt *E. coli* DHFR gene inserted into phage M13mp8. A 25-base oligonucleotide was designed to change the Trp (TGG) codon to His (CAT), and a 26-base oligonucleotide was used to change the Trp to a Phe (TTC). Mutagenesis was carried out as described previously (Villafranca et al., 1983). The entire DHFR genes of both mutants were sequenced by ^{35}S dideoxy sequencing (Sanger et al., 1977, 1980) to verify that only the desired mutation was present. The mutated genes were then cloned from M13mp8 into the plasmid pUC8 and transformed into an *E. coli* cell line in which the chromosomal DHFR gene (*fol*) had been deleted (null allele) and replaced by a kanamycin resistance gene (Howell et al., 1988). This maneuver circumvented the problem of contamination of mutant enzyme with wt DHFR produced by the chromosomal gene.

Cells were grown at 30 °C in a modified version of "terrific broth" (Tartof & Hobbs, 1987) containing 0.017 M KH_2PO_4, 0.072 M K_2HPO_4, 12 g/L bacto-tryptone, 24 g/L bacto-yeast extract, 4 mL/L glycerol, and 2 g/L NaCl. Growth in terrific broth was compared to growth in standard Luria broth (Maniatis et al., 1982) containing 10 g/L bacto-tryptone, 5 g/L bacto-yeast extract, and 10 g/L NaCl. As compared to Luria broth, use of terrific broth resulted in a 3-fold increase in the cell density and a 7–9-fold increase in overall DHFR production. No differences in any properties were seen on comparison of the final purified enzymes from the two sources. Cells were grown to late stationary phase under the selection of 300 μg/mL ampicillin plus 50 μg/mL kanamycin and were lysed by sonication. The cellular lysate was applied to a QAE ZetaPrep 15 disk (LKB), washed with 50 mM KH_2PO_4/1 mM EDTA, pH 8.0, and eluted with the same buffer containing 0.75 M KCl. The mutant DHFRs were then purified to homogeneity as determined by SDS–PAGE by use of Sephadex G-75, (aminohexyl)agarose, and DEAE-Sephadex columns as previously described (Villafranca et al., 1983). Absence of contaminating activity was verified kinetically by use of plots of substrate concentration/velocity as a function of substrate concentration. Such plots show biphasic behavior when contaminating wt enzyme is present (Spears et al., 1971).

Hoping to determine the structural effects of the mutations, we attempted to crystallize the mutant enzymes in binary complexes with MTX, following the same procedure as had been used previously for the wt enzyme (Matthews et al., 1977; Bolin et al., 1982) and other mutants (Howell et al., 1986). Crystals of the W22F·MTX binary complex were formed by vapor diffusion against 23% ethanol. The enzyme was mixed with a 10-fold molar excess of MTX and concentrated to approximately 60 mg/mL (3.3 mM) in a 0.1 M Tris (pH 7.0)/0.05 M histidine (pH 6.8)/0.05 M calcium acetate buffer. Fifteen-microliter drops of this solution were placed on siliconized cover glasses and vapor diffused against a reservoir containing 23% ethanol in 0.1 M Tris, pH 7.0, at 4 °C. Crystals appeared within 3–7 days. The crystals were hexagonal bipyramids, isomorphous with the original wt crystals (space group $P6_1$). X-ray diffraction data were collected on the Mark III multiwire area detector developed at the University of California, San Diego, by Xuong and co-workers (Cork et al., 1973; Xuong et al., 1985) and processed by a suite of programs available at the facility (Anderson, 1987). Crystals were cooled to 4 °C using a wide stream of dry air. A total of 30 609 reflections representing 96% of all unique data were collected to 1.8 Å. The final R_{sym} was 0.049.

The TNT package of programs (version 3E) was used for refinement (Tronrud et al., 1987). The recombinant wt *E. coli* DHFR structure was originally refined using the PROLSQ program to an *R*-factor of 0.163 at 1.9-Å resolution (Howell et al., 1986). Because of slight differences in the geometrical restraints applied by PROLSQ as compared to TNT, the wt structure was re-refined using the TNT programs to an *R*-factor of 0.156 at 1.9-Å resolution. The DHFR structure contains one calcium ion which occupies a space between the two molecules of the crystallographic asymmetric unit and a third symmetry-related molecule. Each molecule of the asymmetric unit also contains one chloride ion located approximately where the 5′-pyrophosphate group of the 2′,5′-diphosphate ADP moiety of the $NADP^+$ is located in the DHFR·$NADP^+$ holoenzyme structure (Bolin et al., 1982; Bystroff et al., 1990). The calcium and two chloride ions, which had been temporarily modeled as sulfur atoms in the PROLSQ refinement, were replaced with the correct ions. The root-mean-square (rms) deviation of bond lengths and bond angles in the final model from their dictionary values was 0.02 Å and 3.0°, respectively.

Observed structure factors for the W22F mutant (F_{mut}) and wt enzyme (F_{wt}), with calculated phases (α_{calcd}), were used as Fourier coefficients for $2F_{mut} - F_{wt}$, α_{calcd} and $F_{mut} - F_{wt}$, α_{calcd} maps. The initial model of the W22F mutant was constructed by fitting a phenylalanine residue at position 22 into these maps with the program FRODO (Jones, 1978) on an Evans and Sutherland PS390 graphics system located at the San Diego Supercomputer Center. Using the TNT program package, a final *R*-factor of 0.161 was obtained for data to 1.9-Å resolution. The rms deviations in bond lengths and bond angles were 0.02 Å and 3.1°.

Although the W22F·MTX complex crystallized readily from pH 7.0, 0.1 M Tris with 23% ethanol, we have been unable to obtain suitably diffracting crystals of the W22H·MTX complex, even after seeding with W22F·MTX or wt·MTX crystals. Attempts at crystallizing the W22H·MTX complex at other pH's from 4.5 to 9.0 also proved unsuccessful.

Ultraviolet difference spectroscopy was performed using split-cell cuvettes in a Perkin-Elmer λ3a spectrophotometer linked to a Perkin-Elmer 3600 data station as previously described (Howell et al., 1986, 1987). Perkin-Elmer programs IFL3 and PECUV were used to collect and analyze the data. Enzyme concentrations were 13–17 μM, and methotrexate

concentrations were 42–50 μM. Equilibrium dialysis experiments to determine K_d values for MTX binding were performed as previously described (Pattishall et al., 1976; Baccanari et al., 1981; Howell et al., 1987).

Steady-state kinetic data were obtained on a Perkin-Elmer λ3b spectrophotometer linked to a Datal 286AT computer. Data were collected and analyzed using the program UVSL3 SCAN/KINETICS (Softways, Moreno Valley, CA 92360). The buffer in all steady-state kinetic experiments was a polybuffer containing 0.033 M succinic acid, 0.044 M imidazole, 0.044 M diethanolamine, and 0.010 M β-mercaptoethanol. This buffer maintains a virtually constant ionic strength (±8%) in the pH range of 4.5–9.5 (Ellis & Morrison, 1982). To eliminate any hysteresis effects (Penner & Frieden, 1985), the enzyme was preincubated with either NADPH or DHF for at least 10 min prior to initiation of the assay. $K_{m(DHF)}$ values were obtained by varying subsaturating concentrations of DHF while maintaining a constant, saturating NADPH concentration of 60 μM. At pH values where saturating concentrations of NADPH were not possible (below pH 5.5 for the W22F and W22H enzymes), $K_{m(DHF)}$ and $K_{m(NADPH)}$ were determined by varying both DHF and NADPH at subsaturating concentrations. The substrate ranges used were 1–100 μM for both DHF and NADPH. Assays were initiated either by the addition of small aliquots of enzyme–NADPH to buffer + DHF or by the addition of enzyme–DHF to buffer + NADPH. The background rate due to decomposition of NADPH, which becomes problematic at low pH (Hillcoat et al., 1967), was accounted for either by subtracting a rate determined from an identical assay done in the absence of enzyme or by using the same initial substrate concentrations in the reference cuvette as in the sample cuvette. Initial rates were obtained in triplicate at least and analyzed by least-squares fitting of the data on substrate concentration/velocity versus substrate concentration plots, as well as by nonlinear regression of substrate concentration versus velocity plots using the program ENZFITTER (Leatherbarrow, 1987). Error analysis of the steady-state kinetic data using the program ENZFITTER gave standard deviations of 1.5%–4.7% on k_{cat} for W22F, 3.4%–5.1% on k_{cat} for W22H at 30 °C, 2.7%–4.5% on k_{cat} for W22H at 12 °C, 6.1%–11.4% on $K_{m(DHF)}$ for W22F, 8.9%–9.8% on $K_{m(DHF)}$ for W22H at 30 °C, 7.0%–13.7% on $K_{m(DHF)}$ for W22H at 12 °C, 7.3%–16.1% on $k_{cat}/K_{m(DHF)}$ for W22F, 11.9%–14.8% on $k_{cat}/K_{m(DHF)}$ for W22H at 30 °C, and 9.7%–18.3% on $k_{cat}/K_{m(DHF)}$ for W22H at 12 °C.

Steady-state kinetic data as a function of pH were fitted to Scheme I (see Figure 4) and eqs 2 and 3 of Howell et al. (1987) by nonlinear least-squares regression analysis designed to minimize the sum of the variations between predicted (pr) and experimentally observed (obsd) values for k_{cat}, $K_{m(DHF)}$, and $k_{cat}/K_{m(DHF)}$ versus pH plots.

$$\sum(k_{cat(obsd)} - k_{cat(pr)})^2 + (K_{m(DHF)(obsd)} - K_{m(DHF)(pr)})^2 + \left(\frac{k_{cat}}{K_{m(DHF)}}^{(obsd)} - \frac{k_{cat}}{K_{m(DHF)}}^{(pr)}\right)^2$$

It is obviously important to have some sort of estimate of the probable error in the derived dissociation constants and kinetic rate constants that were used to fit the pH profiles of Figure 3 before trying to arrive at a functional interpretation. Toward this end the standard deviations of individual k_{cat}, $K_{m(DHF)}$, and $k_{cat}/K_{m(DHF)}$ were used to obtain estimates of their probable maximum and minimum values. For example, the maximum value of k_{cat} at each pH was taken to be the experimentally determined k_{cat} plus its standard deviation. These "altered" data sets of maximum and minimum k_{cat}, $K_{m(DHF)}$, and $k_{cat}/K_{m(DHF)}$, in every combination, were then fitted to the scheme of Figure 4. Differences between the derived constants resulting from the original fitting (with the experimental data) and the largest and smallest derived constants resulting from *any* fitting (with "altered" data sets) were taken as the probable errors for each derived constant listed in Table IV. These error estimates show that some of the derived rate and equilibrium constants, specifically K_y and k_1, are essentially indeterminate, while others can be determined relatively accurately. In Table IV, where two numbers are listed for probable error, the top number represents error in the + direction while the bottom number represents error in the − direction.

Pre-steady-state kinetic measurements were performed on a HI-TECH SF-51 stopped-flow spectrophotometer as previously described (Howell et al., 1990). The pre-steady-state burst of product formation was monitored by following the decrease in fluorescence observed at 450 nm after 290-nm excitation. All experiments were done at 20 °C. Typically, a solution of 30 μM DHFR/250 μM NADPH in one syringe was rapidly mixed with a solution containing 230 μM dihydrofolate in a second syringe. The solutions were buffered at pH 5.6 using 0.025 M acetic acid, 0.025 M MES, 0.050 M Tris, and 0.1 M NaCl.

NADPD was enzymatically prepared from $NADP^+$ (Sigma) by reduction with 1,1-dideuterioethanol (MSD isotopes) catalyzed by *Leuconostoc mesenteroides* alcohol dehydrogenase (Boehringer Mannheim), coupled with aldehyde dehydrogenase (Sigma) to allow nearly complete reaction (Stone & Morrison, 1984; Howell et al., 1987). DHF was prepared by reduction of folic acid with sodium dithionite (Blakley et al., 1960) and stored either in liquid nitrogen or at −20 °C in 5 mM HCl and 50 mM β-mercaptoethanol.

Concentrations were determined spectrophotometrically using molar extinction coefficients of 28 000 M^{-1} cm^{-1} at 282 nm for DHF (Blakley, 1960); 6220 M^{-1} cm^{-1} at 340 nm for NADPH (Penner & Frieden, 1985); and 22 100 M^{-1} cm^{-1} at 302 nm, pH 13, or 23 250 M^{-1} cm^{-1} at 258 nm, pH 13, for MTX (Stone & Morrison, 1986). The molar extinction coefficient used to follow the enzyme reaction was 12 300 M^{-1} cm^{-1} at 340 nm (Baccanari et al., 1975). Enzyme concentrations were obtained by biuret protein determination (Gornall et al., 1949) and by enzyme inhibition titration utilizing MTX (Williams et al., 1979).

Results and Discussion

Binding of Methotrexate. The difference spectra observed when MTX binds to either the W22H or the W22F mutants (data not presented) show no significant changes from either the wt–MTX difference spectrum or the free MTX protonation spectrum (Howell et al., 1986; Poe, 1977). This indicates that MTX is protonated when bound to these mutants, as it is when bound to the wt enzyme. Binding affinities for MTX were determined by equilibrium dialysis with ^3H-labeled MTX. The binary $K_{d(MTX)}$ values at pH 7.0 and 4 °C were found to be 0.12 nM for the W22H enzyme and 0.13 nM for the W22F enzyme, less than twice the previously obtained 0.07 nM for the wt enzyme (Howell et al., 1986). These results indicate there is very little difference in the binding of MTX to the W22H and W22F mutants as compared to the wt enzyme.

X-ray Structure. The difference electron density map for the W22F mutant (Figure 2) shows that the structural effects of the side-chain substitution are localized to the immediate vicinity of the mutation site. The strongest features on the map are near the side chain of residue 22 itself. In molecule 1 of the asymmetric unit two negative peaks are observed at

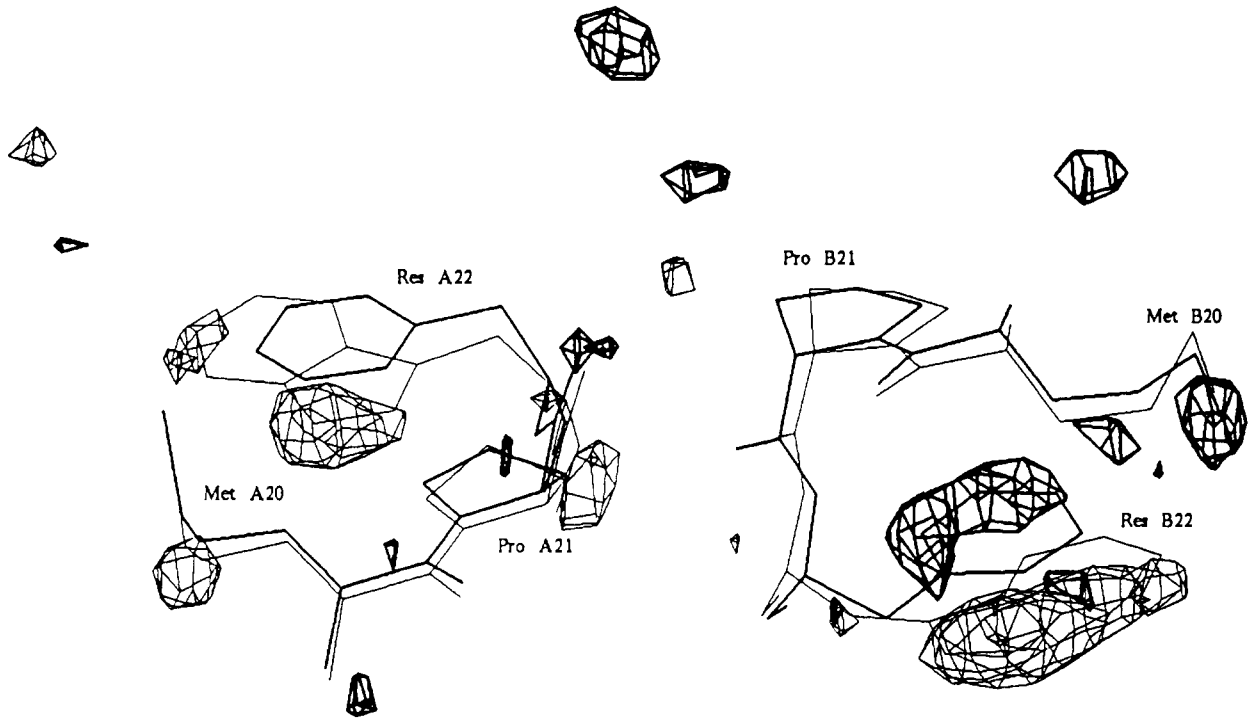

FIGURE 2: The W22F minus wt difference Fourier map contoured at $\pm 4.5\sigma$. Thick contour lines represent positive difference density; thin contour lines represent negative difference density. Residues 20–22 of molecule 1 of the asymmetric unit (labeled with an A) are shown on the left; the same residues of molecule 2 (labeled B) are shown on the right. Res is an abbreviation for the residue at position 22 which is a tryptophan in the wt structure (thin lines) and a phenylalanine in the W22F structure (thick lines).

the periphery of the Trp-22 side chain, close to NE1 and CD1 at one end and the CH2 group at the other. In molecule 2, one large negative peak envelopes the entire five-membered ring of Trp-22 extending to the CH2 and CZ groups of the six-membered ring. In addition, small peaks of difference density occur near the Met-20 side chain in both molecules 1 and 2. The conserved water-403, hydrogen bonded between NE1 of Trp-22 and OD2 of Asp-27 in the wt structure, appears to be unperturbed, as no difference density is observed near it in either of the two DHFR molecules of the asymmetric unit. Thus, water-403 apparently remains bound in the W22F·MTX complex, contrary to the hope and expectation which furnished part of the motivation for constructing this mutant originally.

Relatively small conformational differences between the W22F and wt structures, observed upon crystallographic least-squares refinement, appear to originate at residue 22 and result in an unanticipated movement of the Met-20 side chain. The largest main-chain coordinate shifts occur at CA of residues 22 and 23 in molecule 1, both of which move by 0.6 Å. In addition, CB of Phe-22 has moved 0.8 Å compared with CB of Trp-22 in the wt enzyme, causing the entire side chain to recede slightly into the surface of the enzyme molecule. This movement places the phenylalanine side chain in a more hydrophobic environment than that of the Trp-22 side chain by decreasing contacts with solvent near the surface and increasing van der Waals interactions with apolar groups buried deeper within the protein. This movement of the Phe-22 side chain is accompanied by similar movement of the Met-20 side chain which must shift 0.4 Å to avoid steric overlap with the side chain of Phe-22. A similar movement occurs in molecule 2, although the Phe-22 side chain has adopted a somewhat different position as compared to molecule 1. With respect to the conformation of the wt Trp-22 in molecule 2, this movement is represented by a combined rotation of χ_1 (from 59° to −51°) and χ_2 (from 59° to −38°) and a 0.8-Å movement of CB, as a result of which the Phe-22 benzene ring lies in the same plane as did the wt Trp-22 indole ring but is translated approximately 1.9 Å into the protein surface (see Figure 2). This conformational variability of the Phe-22 side chain, even though its temperature factors are no higher than those for the wt Trp-22 side chain, may indicate increased flexibility. In any case, both phenylalanine side chains in their different conformations are able to maintain many of the same contacts made by the wt Trp-22 side chains. In addition, most atoms of the Met-20 side chain in molecule 2 move as described for molecule 1, with the exception of the SD group which moves 1.0 Å to avoid steric overlap with residues 15 and 16. Despite these movements, van der Waals contact distances between the Met-20 side chain and neighboring side chains and solvent molecules are only slightly altered in both molecules of the asymmetric unit.

To summarize, the most significant conclusions from the structure of the W22F mutant are that (1) fixed water-403 remains in place and (2) the Trp-22 side chain may be important for positioning of the Met-20 side chain (see later discussion of a possible role for Trp-22).

Substrate and Coenzyme Binding Kinetics. Steady-state kinetic analyses show that the two mutant enzymes have only slightly higher $K_{m(NADPH)}$ values as compared to the wt enzyme. At pH 7.0, 30 °C, $K_{m(NADPH)}$ values for W22F and W22H are 2.0 ± 0.4 μM and 1.7 ± 0.3 μM, respectively, in comparison with the previously obtained 0.9 ± 0.4 μM for the wt enzyme (Howell et al., 1986). For the wt and both mutants, $K_{m(NADPH)}$ remains relatively constant throughout the pH range 6–9 but increases below pH 6. In any case $K_{m(NADPH)}$ for the W22F and W22H mutants remains within a factor of 2 of the wt values throughout the measured pH range.

Pre-steady-state analysis of NADPH binding to the W22F mutant shows that the k_{off} and k_{on} rate constants are not greatly affected. Observed values of these rate constants are summarized in Table I. The second-order rate constant for NADPH association, k_{on}, in the W22F mutant is unchanged from that measured with the wt enzyme under the same

Table I: Kinetic Parameters

	pH	wild type	W22F	W22H
k_{cat} (s^{-1})	7.0	29 ± 1[a]	26 ± 0.6	1.9 ± 0.05
$K_{m(DHF)}$ (μM)	7.0	1.1 ± 0.2[a]	18 ± 1	5.3 ± 0.4
$K_{m(NADPH)}$ (μM)	7.0	0.9 ± 0.4[a]	2.0 ± 0.4	1.7 ± 0.3
$k_{cat}/K_{m(DHF)}$ (s^{-1} μM^{-1})	7.0	26 ± 5[a]	1.4 ± 0.08	0.36 ± 0.03
$k_{cat}/K_{m(NADPH)}$ (s^{-1} μM^{-1})	7.0	32 ± 14[a]	13 ± 3	1.1 ± 0.2
pK (k_{cat})		8.2 ± 0.2	6.5 ± 0.1	7.3 ± 0.3
pK ($k_{cat}/K_{m(DHF)}$)		8.0 ± 0.2	5.8 ± 0.1	7.3 ± 0.3
k_{on}(NADPH) (s^{-1} μM^{-1})	8.0	15.1 ± 0.9[b]	14.6 ± 2.9	
k_{off}(NADPH) (s^{-1})	7.7	4.4 ± 0.2[c]	8.4 ± 1.4	
k_{off}/k_{on}(NADPH) (μM)	8.0	0.29 ± 0.02	0.58 ± 0.15	
k_{off}(NADP$^+$) (s^{-1})	7.8	99 ± 3	167 ± 14	
k_{on}(DHF) (s^{-1} μM^{-1})	8.0	40 ± 6[d]	19.8 ± 3.6	
k_{off}(DHF) (s^{-1})	7.7	13 ± 1[e]	39 ± 2	
k_{off}/k_{on}(DHF) (μM)	8.0	0.32 ± 0.05	1.97 ± 0.37	
$k_{hydride}$ (s^{-1})	5.6	730 ± 70	260 ± 33	5.6 ± 1.3
pK ($k_{hydride}$)		6.4 ± 0.13	5.9 ± 0.16	

[a] From Howell et al. (1990). [b] Compares with 12 ± 1 from Fierke et al. (1987); measured at pH 9.0. [c] Compares with 2 ± 1 from Fierke et al. (1987); measured at pH 9.0. [d] From Fierke et al. (1987); measured at pH 9.0. [e] Compares with 39 ± 9 from Fierke et al. (1987); measured at pH 9.0.

conditions, while the dissociation rate constant for NADPH, k_{off}, is slightly higher with the W22F enzyme than with the wt enzyme. The kinetic ratio of k_{off}/k_{on} is thus slightly higher in the W22F enzyme than in the wt enzyme. Because the relationship between the k_{of}/k_{on} ratio and K_d is dependent on the relative concentrations of two enzyme conformations, only one of which binds NADPH [Scheme I in Fierke et al. (1987)], and the equilibrium constant between these two conformations is $\approx$1 for both the wt (Cayley et al., 1981; Fierke et al., 1987) and the W22F enzyme (M. Farnum, unpublished results), the thermodynamic $K_{d(NADPH)}$ is actually twice the k_{off}/k_{on} ratio for both enzymes [eq 1 in Fierke et al. (1987)]. Thus, the thermodynamic $K_{d(NADPH)}$ values are 0.58 μM for the wt and 1.1 μM for the W22F enzyme. The dissociation rate constant for NADP$^+$ is also slightly higher in the W22F enzyme than in the wt enzyme (Table I).

Although the mutations do not have much effect on NADPH binding, they have appreciably altered $K_{m(DHF)}$ and k_{cat} from those of the wt enzyme. Steady-state kinetic parameters for the W22F, W22H, and wt enzymes obtained at pH 7.0, 30 °C, are given in Table I. Although the W22F mutation has little effect on k_{cat} at pH 7.0, the increase observed in K_m for DHF has led to an 18-fold decrease in $k_{cat}/K_{m(DHF)}$ at pH 7.0. The W22H mutation, however, affects both k_{cat}, which is 15-fold lower in the mutant enzyme than in the wt, and $K_{m(DHF)}$, which is 5-fold higher in the mutant than in the wt enzyme.

The dissociation constant for DHF, $K_{d(DHF)}$, has also increased in the W22F mutant as compared to wt DHFR. The off rate for DHF is 39 s^{-1} for the W22F enzyme, a 3-fold increase over the wt value of 13 s^{-1}. The value of k_{on} in the W22F enzyme is about half of that of the wt. The ratios of k_{off}/k_{on} for DHF dissociation from the wt and W22F enzymes are thus 0.32 μM and 2.0 μM, respectively. For comparison, $K_{m(DHF)}$ values are 1.5 μM and 24 μM for wt and W22F DHFR, respectively, at pH 8.

The kinetic properties of the *E. coli* W22F and W22H mutant enzymes are similar to those seen in human and mouse DHFRs in which the equivalent tryptophan has been mutated, although they contrast with a similar mutation in the *Lactobacillus casei* DHFR (Beard et al., 1991; Huang et al., 1989; Thillet et al., 1988; Andrews et al., 1989). Table II contains the parameter ratios of mutant to wt for each species. Both DHF and NADPH binding appear to be different in the *L. casei* mutant from any of the other mutants. All of the mutations except for that in the *L. casei* enzyme only slightly alter NADPH binding, and all of the mutations except that in *L. casei* increase $K_{m(DHF)}$. While the *E. coli* W22F and W22H mutations, the Trp-24 → Phe mutation in the human enzyme (h:W24F), and the Trp-24 → Arg mutation in the mouse enzyme (m:W24R) only slightly affect NADPH binding, the Trp-21 → Leu mutation in the *L. casei* enzyme (lc:W21L) causes a 420-fold increase in the k_{off}/k_{on} ratio for NADPH. The *E. coli* W22F and W22H mutations, as well as the h:W24F and m:W24R mutations, all increase $K_{m(DHF)}$ by 4.4–110-fold. The lc:W21L mutant, however, actually decreases $K_{m(DHF)}$ by 120-fold.

Table II: Effect of Trp-22 Mutations in Various DHFRs[a]

	E. coli W22H	*E. coli* W22F	human W24F[b]	mouse W24R[c]	*L. casei* W21L[d]
k_{cat}	0.063	0.87	3.2	0.028	0.14
$K_{m(NADPH)}$	1.9	2.2	0.81, 21[e]	1.7	
k_{off}/k_{on}(NADPH)		2.0	2.2		420
$K_{m(DHF)}$	4.4	15	25	110	0.008
k_{off}/k_{on}(DHF)		6.2	4.4		5.1
$k_{hydride}$	0.0077	0.36	0.065		

[a] Numbers are the ratios of mutant to wild-type parameter for each species. [b] From Beard et al. (1991). [c] From Thillet et al. (1988). [d] From Andrews et al. (1989). [e] From Beard et al. (1991); two different values of $K_{m(NADPH)}$ for the human wild type are reported.

The Trp-22 residue in the *E. coli* DHFR·folate·NADP$^+$ crystal stucture interacts both with folate, through hydrogen bonds with water-403, and with NADP$^+$, by way of van der Waals contacts. The W22F·MTX crystal structure shows that the effects of this mutation are minimal and primarily occur at the folate binding site. In contrast, NMR studies on the *L. casei* lc:W21L enzyme indicate that the major structural change is that the nicotinamide ring of NADPH binds differently (Birdsall et al., 1989). Perhaps a Trp → Leu substitution produces effects different from a Trp → Phe substitution.

Pre-Steady-State Burst Kinetics. Rates of the pre-steady-state burst phase of product formation were compared for the wt and mutant enzymes. For the wt, our results are in agreement with those of Fierke et al. (1987), who obtained a pH-independent rate constant for hydride transfer of 950 s^{-1}. However, at pH 5.6 the observed hydride-transfer rate of 730 s^{-1} observed for the wt decreases to 260 s^{-1} for the W22F mutant and to 5.6 s^{-1} for the W22H mutant (see Table I). Thus, while the hydride-transfer rate for W22F is reduced by only a factor of 2.8 in comparison to the wt, W22H has been slowed by a factor of 130.

Deuterium Isotope Effects. Primary deuterium isotope effects on steady-state kinetic parameters can indicate whether hydride transfer is at least partially rate limiting. The results of Chen et al. (1987) and Fierke et al. (1987) show that the rate of hydride transfer is not limiting in the steady state for the wt enzyme at pH 7.0 and below since $^DV(k_{cat(NADPH)}/k_{cat(NADPD)})$ approaches 1. Instead, the rate of product (THF) release limits the observed maximum velocity of the wt enzyme at neutral and acidic pH. However, at pH 9 ^DV increases to 2.7, indicating that hydride transfer becomes more nearly rate limiting at alkaline pH owing to the decreased concentration of protonated enzyme-bound substrate (DHF).

For the W22F and W22H mutants, primary deuterium isotope effects (Table III) reveal that hydride transfer is rate

Table III: pH Dependence of Deuterium Isotope Effects

enzyme	pH	^{D}V	$^{D}(V/K_{m(DHF)})$
	6.0[a]	1.0	nd[c]
wild type	7.0[b]	1.1	nd
	9.0[a]	2.7	3.0
	5.1	3.8	3.1
W22H	6.9	3.6	3.7
	8.9	3.4	3.7
	5.1	1.7	2.0
W22F	6.9	3.0	3.4
	8.9	3.2	3.5

[a] From Chen et al. (1987). [b] From Mayer et al. (1986). [c] nd, not determined.

limiting in at least part of the pH range examined. The W22H mutant shows a full[4] deuterium isotope effect (>3) throughout the experimental pH range, indicating that hydride transfer is nearly fully rate determining at all pH values. Direct measurement of the hydride-transfer rate at pH 5.6 gives 5.6 s^{-1}, only slightly higher than the k_{cat} of 3.1 s^{-1} at the same pH. The pH dependence of the isotope effect is more complex for the W22F mutant, however. A full isotope effect is seen at and above pH 7, but at pH 5 ^{D}V is only 1.7, suggesting that hydride transfer is only partially rate determining at low pH. Direct measurement of the hydride-transfer rate at pH 5.6 yields 260 s^{-1}, compared to the k_{cat} of 82 s^{-1}. As the pH is lowered below pH 5, ^{D}V also continues to decrease for the W22F enzyme, although problems with the assay below this pH make it very difficult to determine values accurately. At low pH both the insolubility of DHF (Kaufman & Gardiner, 1966) and the acid-catalyzed hydration of NADPH (Oppenheimer & Kaplan, 1974; Johnson & Tuazon, 1977) interfere with the assay.

pH Dependence of k_{cat} and $k_{cat}/K_{m(DHF)}$. The pH dependence of k_{cat} and $k_{cat}/K_{m(DHF)}$ for the wt enzyme and for the W22H and W22F mutants is illustrated in Figure 3. The curves in Figure 3 were calculated by selecting best-fit derived rate and equilibrium constants defined according to the protonation scheme given in Figure 4, as detailed in the following section. k_{cat} for the W22F mutant attains a maximum value of 93 s^{-1} at pH 5.0, about 5-fold higher than for the wt enzyme at the same pH (20 s^{-1}) and almost 3-fold higher than the maximal value of k_{cat} (36 s^{-1} at pH 6.5) observed for the wt enzyme. Although the hydride-transfer rate for the W22F mutant is lower by a factor of 2.8 as compared to that for the wt at pH 5.6, the W22F k_{cat} is elevated by a factor of 3 as compared to the wt. This result indicates that the rate-limiting step for the wt enzyme, THF release, has been accelerated by the mutation—not surprising since the W22F mutant binds DHF less tightly than the wt, with k_{off} increased about 3-fold. Although the W22F mutant has a higher k_{cat} than the wt below pH 6.8, it nonetheless is less efficient than the wt enzyme because of its increased $K_{m(DHF)}$. Unlike the W22F mutant, the W22H mutant remains less active than the wt enzyme throughout the observed pH range. The k_{cat} value for W22H is 4 s^{-1} at pH 5.0, over 20-fold slower than W22F and 5-fold slower than the wt at this pH.

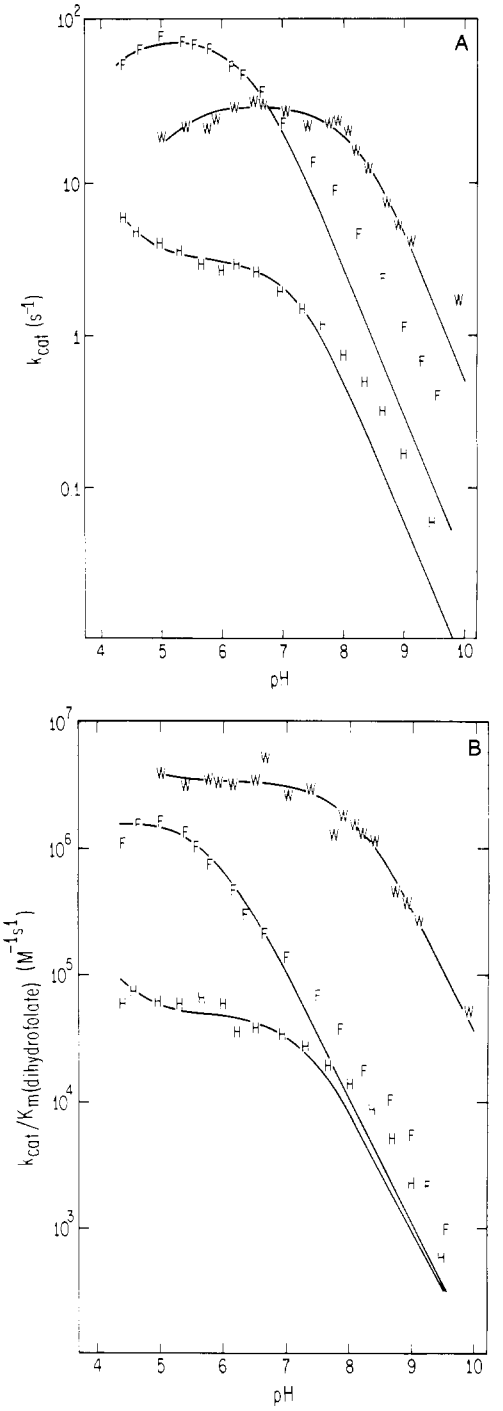

FIGURE 3: Steady-state pH profiles of (A) k_{cat} and (B) $k_{cat}/K_{m(DHF)}$ for wt DHFR (W), W22F DHFR (F), and W22H DHFR (H). The curves were fitted to eq 2 and 3 from Howell et al. (1987), relating to the scheme presented in Figure 4, as described in the text.

While the wt enzyme exhibits a kinetic pK of 8.2 in its k_{cat} profile (Howell et al., 1986), the W22F and W22H mutants show decreased kinetic pK's of 6.5 and 7.3, respectively. In the $k_{cat}/K_{m(DHF)}$ profiles, pK's are 8.0 for the wt, 5.8 for W22F, and 7.3 for W22H. In the case of the wt enzyme, these observed kinetic pK's are only apparent pK's, arising from a change in the rate-determining step from THF release at low pH to hydride transfer at high pH for the k_{cat} profile and nonequilibrium binding of DHF for the $k_{cat}/K_{m(DHF)}$ profile (Fierke et al., 1987). Direct measurement of the hydride-

[4] How large should ^{D}V be for hydride transfer to be considered fully rate determining? In the case of DHFR, several lines of evidence show that the maximal value of ^{D}V lies between 3.0 and 3.8. Direct measurement of the rate of hydride transfer shows a deuterium isotope effect of 3 between pH 5.0 and 8.0 (Fierke et al., 1987). Steady-state rate constants for wt DHFR at high pH, where hydride transfer is thought to be rate determining, show a ^{D}V of 3 as well (Chen et al., 1987). Previously studied mutant DHFRs in which hydride transfer has been slowed sufficiently to become rate limiting show steady-state ^{D}V values of 3.0–3.3 (Howell et al., 1987). Also, a ^{D}V of 3.8 is observed in an enzymic reduction of an imine by NADH utilizing glutamate dehydrogenase, suggesting that low intrinsic primary isotope effects in reductase/dehydrogenase-catalyzed reactions are not confined to DHFR (Srinivasan & Fisher, 1985).

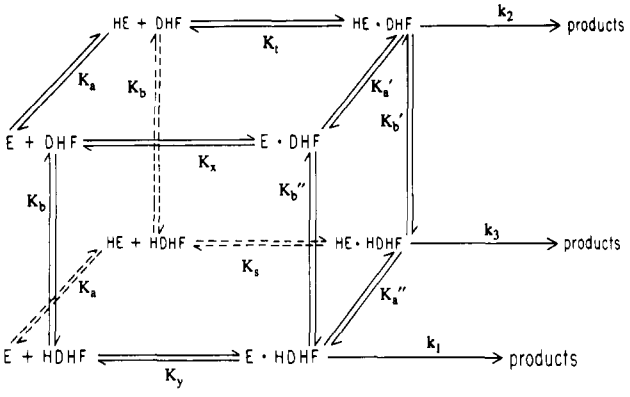

FIGURE 4: Kinetic scheme for DHFR, from Howell et al. (1987). K_a, K_a', K_a'', K_b, K_b', and K_b'' are acid dissociation constants; K_s, K_t, K_x, and K_y are dissociation constants of the substrate from the DHFR·NADPH·DHF complexes; and k_1, k_2, and k_3 are catalytic rate constants. Best-fit parameters are given in Table IV.

transfer rate vs pH yields a pK of 6.5 (Fierke et al., 1987), presumably the true pK of Asp-27 in the wt enzyme. Several other methods have also been used previously to determine the true pK of Asp-27 in the wt enzyme, yielding values of 6.3–6.7 (Cayley et al., 1981; Stone & Morrison, 1983). For the W22F mutant, the observed pK of 6.5 seen in the k_{cat} vs pH profile is probably slightly higher than the true pK of Asp-27 as both hydride transfer and product release contribute to the rate-limiting step, although the change in the rate-limiting step is not as pronounced in the W22F mutant as in the wt enzyme. Indeed, direct measurement of the hydride-transfer rate vs pH yields a pK of 5.9 for the W22F mutant. For the W22H mutant, the kinetic pK of 7.3 probably represents a true pK, as the rate-limiting step for this mutant enzyme does not change in the observed pH range. However, whether this pK represents an elevated pK for Asp-27 or titration of His-22 is unclear.

In all four k_{cat} and $k_{cat}/K_{m(DHF)}$ vs pH curves for W22H and W22F, the best-fit profiles decrease faster as pH increases than the actual data profile does. That is, at pH values above the kinetic pK, the observed steady-state kinetic parameters fall off with a slope that is somewhat shallower than the expected slope of −1.0. In Figure 3, the predicted best-fit curves above the kinetic pK are calculated with the expected slope of −1.0, while the actual data points clearly have a more shallow slope. Similar results have been seen previously for several other mutant DHFRs (Howell et al., 1986, 1987; Murphy & Benkovic, 1989). In order to confirm the pK values and determine the slopes of the kinetic profiles above the pK's, steady-state kinetic data were fitted (by nonlinear least-squares regression) to simple titration equations corrected for slope using the equation given in Murphy and Benkovic (1989). For W22F above pH 5, the k_{cat} vs pH data fit well to a single titration with a pK of 6.5, using 94 s^{-1} as the maximal value of k_{cat} and a slope of −0.74, while the $k_{cat}/K_{m(DHF)}$ vs pH data are best fitted with a pK of 5.8, maximal value of $k_{cat}/K_{m(DHF)}$ of 14×10^6 M^{-1} s^{-1}, and slope of −0.75 (data not shown). Similarly, both W22H plots above pH 5.5 fit well to a pK of 7.3, using 3.2 s^{-1} as the maximal value of k_{cat} and a slope of −0.73, while the $k_{cat}/K_{m(DHF)}$ data fit best with 0.57×10^6 M^{-1} s^{-1} as the maximal value and −0.71 as the slope (data not shown).

The cause of these shallower than expected slopes is unknown. Perhaps they are due to some degree of enzyme-catalyzed hydride transfer without protonation of N5, leading to higher than predicted rates at pH values above the pK of Asp-27. Such a possibility could be incorporated into our protonation scheme (Figure 4; see next section) by including an additional step proceeding from E·DHF to products with a corresponding rate constant, but we felt that further elaboration of the scheme was not justified by the data.

For the wt enzyme, k_{cat} decreases somewhat as the pH is lowered below pH 6.5, and similarly for the W22F mutant, k_{cat} decreases below pH 5. In contrast, however, k_{cat} for the W22H mutant continues to slowly increase as the pH is lowered below pH 5. A possible concern is that this low-pH behavior may be an artifact due to enzyme inhibition by impurities in commercial preparations of NADPH, since a problem of this kind has been reported for *L. casei* DHFR (Andrews et al., 1989). To examine this question, NADPH was repurified by FPLC on a Mono Q column (Orr & Blanchard, 1984), and kinetic parameters were remeasured at pH 5.0 and 7.0 for the wt enzyme. Both k_{cat} and $k_{cat}/K_{m(DHF)}$ were were within 2% of those determined with unpurified NADPH (data not shown). Thus, any impurities present in our sample of NADPH are not affecting steady-state kinetic measurements on *E. coli* wt DHFR.

Interpretation of Steady-State Parameter vs pH Profiles. One way to analyze the observed pH dependencies of the steady-state kinetic parameters is by using the protonation scheme of Figure 4 [Scheme I of Howell et al. (1987)]. The dissociation constants and rate constants used in this scheme are as follows, with DHF and HDHF representing unprotonated and N5-protonated substrate, and E and HE representing unprotonated and protonated holoenzyme, that is, enzyme complexed with NADPH. In this scheme K_a and K_b represent the acid dissociation constants of the enzyme (presumably Asp-27) and substrate DHF; K_a' and K_a'' represent acid dissociation constants of the enzyme with bound unprotonated substrate DHF and bound N5-protonated substrate, HDHF; K_b' and K_b'' represent acid dissociation constants of substrate when bound to protonated and unprotonated enzyme; K_s, K_t, K_x, and K_y are dissociation constants of substrate from HE·HDHF, HE·DHF, E·DHF, and E·HDHF; and k_1, k_2, and k_3 are rate constants for the formation of product from E·HDHF, HE·DHF, and HE·HDHF. Because these rate and equilibrium constants are not directly measurable, but rather are derived from the Figure 4 protonation scheme, they will be called "derived rate and equilibrium constants" to avoid confusion with the directly measurable kinetic constants. In Figure 3 the observed pH dependencies of the steady-state kinetic parameters are fitted to the protonation scheme of Figure 4. The data were fitted to eq 2 and 3 of Howell et al. (1987) by nonlinear least-squares regression analysis designed to minimize the sum of the squares of the variations from the k_{cat} and $k_{cat}/K_{m(DHF)}$ data points shown in Figure 3 as well as the $K_{m(DHF)}$ data (not shown). K_b was held constant at the value reported for the acid dissociation constant of N5 of DHF (Maharaj et al., 1990) while the rest of the derived rate and equilibrium constants from these equations were systematically varied from initial estimates. This procedure was repeated by computer until a 0.1% change in any derived rate or equilibrium constant failed to improve the fitting. Since the pK_a values of the enzymes (5.8–8.0) are considerably higher than pK_b of DHF (2.6), the concentration of E·HDHF will be very small relative to the other species represented in the scheme of Figure 4. As a result, K_y and k_1 are relatively unimportant in fitting the kinetic data to this scheme and are essentially indeterminate. The best-fit values of the derived rate constants that could be determined (k_2, k_3, K_s, K_t, K_x, and K_a) for the wt, W22F, and W22H enzymes are given in Table IV.

Table IV: Derived Rate and Equilibrium Constants

footnotes	constant	wild type 30 °C	W22F 30 °C	W22H 30 °C	W22H 12 °C
a	pK_a	8.0 ± 0.2	5.8 ± 0.2	7.3 ± 0.2	7.0 ± 0.2
b	pK_a'	8.2 ± 0.2	6.5 ± 0.2	7.3 ± 0.2	7.2 ± 0.2
c	pK_b	2.6	2.6	2.6	2.6
d	pK_b'	5.1 ± 0.2	4.0 ± 0.3	2.6 ± 0.3	3.4 ± 0.2
e	K_s (μM)	$0.0033 \pm \frac{0.0009}{0.0005}$	$0.23 \pm \frac{0.13}{0.06}$	$6.4 \pm \frac{3.8}{1.1}$	$0.50 \pm \frac{0.18}{0.12}$
f	K_t (μM)	$0.99 \pm \frac{0.09}{0.06}$	$5.8 \pm \frac{2.1}{0.9}$	$6.4 \pm \frac{0.6}{0.6}$	$3.1 \pm \frac{0.2}{0.2}$
g	K_x (μM)	$1.6 \pm \frac{0.7}{0.2}$	$26 \pm \frac{1}{3}$	$6.1 \pm \frac{1.8}{0.3}$	$5.1 \pm \frac{1.5}{0.5}$
h	k_2 (s^{-1})	$33 \pm \frac{3}{3}$	$98 \pm \frac{5}{5}$	$3.2 \pm \frac{0.3}{0.6}$	$0.98 \pm \frac{0.06}{0.16}$
i	k_3 (s^{-1})	$5.0 \pm \frac{2.0}{0.3}$	$0.01 \pm \frac{0.08}{0.004}$	$160 \pm \frac{4000}{140}$	$5.0 \pm \frac{18}{1.1}$

[a] From E ⇌ HE. [b] Calculated from $K_a' = K_aK_t/K_x$, E·DHF ⇌ HE·DHF. [c] From Maharaj et al. (1990); DHF ⇌ HDHF. [d] Calculated from $K_b' = K_bK_s/K_t$, HE·DHF ⇌ HE·HDHF. [e] HE + HDHF ⇌ HE·HDHF. [f] HE + DHF ⇌ HE·DHF. [g] E + DHF ⇌ E·DHF. [h] HE·DHF →. [i] HD·HDHF →.

In order to confirm that the values of the derived equilibrium constants are reasonable, they can be compared to the $K_{m(DHF)}$ values. While $K_{m(DHF)}$ is not equal to $K_{d(DHF)}$ in the ternary complex, it does give some idea of what $K_{d(DHF)}$ might be. At high pH, above the pK_a and pK_b, most of the enzyme and substrate will be unprotonated and therefore the dissociation constant of DHF will be approximately equal to K_x in Figure 4. At pH 9.0, the observed $K_{m(DHF)}$ for wt, W22F, W22H (at 30 °C), and W22H (at 12 °C) are 1.5 μM, 22 μM, 7.5 μM, and 6.0 μM, all within 20% of the derived K_x values. As a further check, at pH values between the pK_a and pK_b most of the enzyme will be protonated while most of the substrate will be unprotonated; therefore, the dissociation constant of DHF will approximate K_t. At pH 5.0, the observed $K_{m(DHF)}$ for wt, W22F, W22H (at 30 °C), and W22H (at 12 °C) are 0.52 μM, 5.4 μM, 7.0 μM, and 3.0 μM. With the exception of the wt, all are within 10% of the derived K_t values. As additional verification the derived best-fit values of pK_a can be compared with the kinetic p*K*'s observed in the $k_{cat}/K_{m(DHF)}$ vs pH profiles (which correspond to ionizations of the enzyme·NADPH complexes), and in all cases they are equal. The cyclical nature of the equilibria in Figure 4 allow us to calculate K_a' from the relationship $K_a' = K_aK_t/K_x$. All resulting derived values of pK_a' are equal to the kinetic p*K*'s observed in the k_{cat} vs pH profiles, which correspond to ionizations of the enzyme·DHF·NADPH complexes (Fersht, 1985).

Is it possible that the ionization constant of DHF is altered upon binding to the enzyme? Since $K_a \neq K_a'$ for the wt or W22F enzymes, it appears that the p*K* of enzyme might be altered upon binding of substrate, so perhaps the p*K* of substrate could be altered by binding as well. The cyclical nature of the equlibria in Figure 4 can be used to calculate the ionization constant of bound DHF (K_b') using the relationship $K_b' = K_bK_s/K_t$. From the reported value of K_b (Maharaj et al., 1990) and the derived values of K_s and K_t, the calculated values of K_b' are 5.1 ± 0.2 when bound to the wt enzyme and 4.0 ± 0.3 when bound to the W22F mutant enzyme. Although the best-fit derived values imply that the ionization constant for N5 of DHF may be elevated when bound to the wt or W22F enzymes, it must be stressed that there is no structural evidence to support this. When DHF is bound in the ground state, N5 is surrounded by hydrophobic side chains (notably Met-20) which should, theoretically, decrease the pK_b'. One would not expect a positively charged N5 to be stabilized by a hydrophobic environment. Nevertheless, mechanistically, at some point in the catalytic reaction pathway between the ground state and the formation of products, N5 must be protonated. Of the three DHFR variants studied, the one with the highest apparent elevation of pK_b' (wt) is also the one with the highest hydride-transfer rate, while the enzyme with the lowest apparent elevation of pK_b' (W22H) is the one with the lowest hydride-transfer rate. Thus, it appears that the ionization constant of DHF upon binding to the wt or the W22F mutant may be elevated from 2.59 to 5.1 or 4.0, respectively, facilitating protonation at N5 of DHF. When bound to the W22H mutant, however, the ionization constant of DHF is essentially unchanged from its solution value.

Yet another puzzling result for the wt and W22F enzymes arising from the derived equilibrium constants is that $K_s < K_t < K_x$. In effect, these enzymes appear to bind protonated DHF much more tightly than unprotonated DHF in the Michaelis complex. However, once again, there is no structural evidence to suggest how this might occur. On the contrary, the fact that N5 is surrounded by hydrophobic groups would suggest that unprotonated DHF should be the more tightly bound form. Mechanistically, however, if the transition state is indeed protonated at N5, perhaps $K_s < K_t < K_x$ simply implies that as the bound complex more closely resembles the transition state, binding becomes tighter. The very slow derived rates for HE·HDHF (k_3) as compared to HE·DHF (k_2) in these enzymes does indicate that catalyzed reduction of pre-protonated substrate is less effective than catalyzed reduction of bound, unprotonated substrate. Therefore, in order to maximize the turnover rate, wt and W22F DHFR must bind and utilize unprotonated DHF, using the increased binding energy upon protonation to stabilize the transition state as opposed to the ground state. In other words, tighter binding of pre-protonated DHF may be due to its mimicking the transition state, with the low turnover rate in such complexes resulting from unproductive tight binding in the ground state. Therefore, while the enzyme binds protonated substrate more tightly than unprotonated substrate, it would not be advantageous to elevate the pK_b' of DHF bound to the enzyme too much, as this would trap the enzyme in a less productive complex. The low turnover rates of complexes in which pre-protonated DHF is bound also explains the decrease in k_{cat} for the wt enzyme below pH 6, and the decrease in the W22F k_{cat} below pH 5. This decrease in k_{cat} may provide evidence for the existence of a hypothetical transiently bound water molecule that hydrogen bonds simultaneously to O4 and N5 of DHF [Figure 6 from Bystroff et al. (1990)]. If this transient water molecule were bound in the ground state, and pre-protonation of substrate occurred, the enzyme would fall

into a thermodynamic free energy hole. By leaving protonation to a transient process, the enzyme can fully utilize all of the binding energy in the transition state to enhance catalysis.

Peculiarities of W22H Kinetics. The shapes of the W22H $k_{cat}/K_{m(DHF)}$ and k_{cat} vs pH profiles at low pH are unusual. Unlike the wt or W22F, the activity of the W22H mutant does not decrease below pH 6 but actually increases. This is apparent in the k_{cat} vs pH profile, although it is questionable in the $k_{cat}/K_{m(DHF)}$ vs pH profile (Figure 3). It is unclear what may cause this effect, although there are at least three possibilities. First, the W22H mutant may be using preprotonated substrate in the same way as does the Asp-27 → Ser mutant (Howell et al., 1986), with the effect only becoming evident at sufficiently low pH. Second, the increase in activity below pH 5.5 could indicate the presence of a second group in the active site of the enzyme whose protonation state influences enzyme activity, i.e., the His-22 residue. Experiments by Howell et al. (1987) have shown that a prototropic group located in the general vicinity of Asp-27 but at a different position is capable of contributing to substrate protonation. Finally, the shape of the profiles may be due to a kinetic "hollow" effect. Kinetic hollows are dips in such pH profiles in the vicinity of a kinetically observed pK and are observed only when the substrate and the proton are both sticky (Cleland, 1977). While reports of hollows have been infrequent, such an effect has been observed previously in an *E. coli* DHFR mutant in which Phe-31 was replaced by a tyrosine (Chen et al., 1987). Possibly of diagnostic value, it is noteworthy that kinetic hollows have been observed to be temperature dependent, becoming more pronounced at lower temperatures (Cook et al., 1981). In order to further investigate this question, k_{cat} and $k_{cat}/K_{m(DHF)}$ vs pH profiles for W22H were determined at a lower temperature, 12 °C.

A comparison of the pH dependence of k_{cat} and $k_{cat}/K_{m(DHF)}$ for the W22H mutant at 12 °C and 30 °C is shown in Figure 5. Low-pH kinetic parameters are much easier to determine at lower temperatures owing to the decreased decomposition rates of NADPH at 12 °C as compared with at 30 °C. These data clearly show an increase in both k_{cat} and $k_{cat}/K_{m(DHF)}$ below pH 5. The values of k_{cat} and $K_{m(DHF)}$ at 12 °C are decreased by factors of 4 and 2, respectively, compared to the values determined at 30 °C. Derived rate and dissociation constants that give a best fit to the scheme of Figure 4 for the W22H enzyme at 12 °C are given in Table IV.

We conclude that the unusual shapes of the W22H k_{cat} and $k_{cat}/K_{m(DHF)}$ vs pH profiles are unlikely to be the result of a kinetic hollow. Comparison of these kinetic profiles at 12 and 30 °C (Figure 5) shows that temperature does not alter the profile shapes. Also, there is no evidence that DHF is a sticky substrate for the W22H enzyme. In fact, $K_{m(DHF)}$ is elevated 5-fold in the W22H mutant compared to in the wt enzyme, suggesting that DHF binding is weaker in this mutant. The 130-fold decrease in the hydride-transfer rate caused by the W22H mutation also suggests that catalysis is quite slow relative to the rate of diffusion of DHF into the enzyme's binding site, thus providing more evidence that DHF is not a sticky substrate. Therefore, the increase in activity seen in the W22H pH profiles cannot be attributed to a kinetic hollow effect.

Since a kinetic hollow is not responsible for the increase in W22H activity below pH 5, this increase must be due to a second kinetic pK. The W22H k_{cat} profiles clearly show an increase in activity below pH 5, although even at the lower temperature it is still not feasible to measure kinetic parameters below pH 4. Thus, we cannot determine the value of the

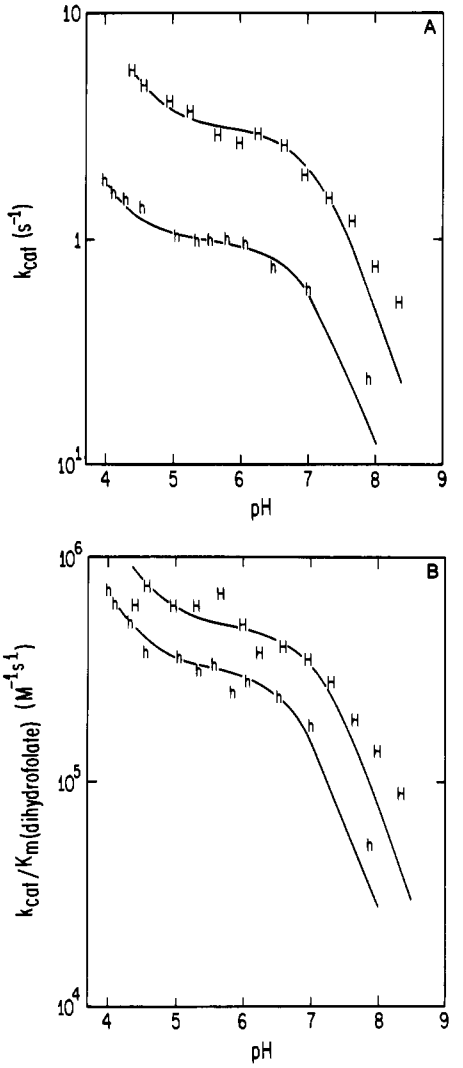

FIGURE 5: Steady-state pH profiles of (A) k_{cat} and (B) $k_{cat}/K_{m(DHF)}$ for W22H DHFR at 30 °C (H) and 12 °C (h). The curves were fitted to eq 2 and 3 from Howell et al. (1987), describing the scheme presented in Figure 4, as described in the text.

kinetic pK associated with the increase in activity below pH 5 (although it is certainly < 4), and so we cannot say whether this increase in activity might be due to turnover of preprotonated substrate, which should show a kinetic pK equal to the pK of free DHF (Maharaj et al., 1990), or, alternatively, whether it might be due to a second prototropic group (His-22 or Asp-27) contributing to substrate protonation.

Still unresolved is the question of whether the kinetic pK of 7.0–7.3 seen in the W22H profiles represents a titration of Asp-27 or His-22. While the presence of an unprotonated, uncharged His-22 might increase the pK of Asp-27 from its normal value of 6.5 in the wt to 7.0–7.3 in the W22H enzyme, it seems unlikely since the His-22 is replacing a more hydrophobic tryptophan. Alternatively, a protonated, positively charged His-22 with a pK of 7.0–7.3 could decrease the pK of Asp-27 to <4. In this case, the increase in activity seen below pH 5 may represent a contribution to catalysis from a protonated Asp-27 residue with pK < 4, while at higher pH it is not Asp-27 but rather the protonated His-22 residue that catalyzes substrate protonation. Returning to our protonation scheme (Figure 4), if the higher pK of 7.0–7.3 corresponds to His-22 and the lower pK of <4 corresponds to Asp-27, the catalysis associated with the derived rate constant k_2 would result from His-22-catalyzed protonation (since the acid dissociation constant K_a is associated with the higher pK of

7.0–7.3). Additionally, if the second proton in this scheme (K_b) is not entirely due to DHF pre-protonation (pK = 2.6) but rather represents some contribution from Asp-27 with pK < 4, the catalysis associated with the derived rate constant k_3 might result, at least partially, from Asp-27-mediated substrate protonation. Perhaps this explains the large value of k_3 in the W22H enzyme relative to those of the wt or W22F enzymes (Table IV). In effect, k_3 in the W22H might represent what k_2 represents in the wt and W22F enzymes.

A Possible Role for Trp-22 in Catalysis. Both mutations at Trp-22 decrease the rate of hydride transfer, the W22F mutation by a factor of 2.8 and the W22H mutation by a factor of 130. Evidently the Trp-22 side chain plays some role in maintaining optimum transition-state binding. We suggest that role may be to aid in correctly positioning the side chain of Met-20 (or the functionally equivalent hydrophobic side chain in other species of DHFR) with respect to N5 of substrate DHF. The side chain of Trp-22 is seen to make van der Waals contacts with Met-20 in both the DHFR·MTX binary and DHFR·folate·NADP$^+$ ternary complexes, though not in exactly the same way. Moreover, the structure of the W22F mutant reported here shows that even the relatively conservative substitution of a benzene ring for the indole ring of Trp-22 perturbs the position of the Met-20 side chain by 0.4 Å. The smaller, more polar W22H substitution is likely to perturb the Met-20 side chain even more, particularly when it is protonated at low pH. It is conceivable that the amphipathic side chain of Trp-22 is needed to simultaneously hydrogen bond with water-403 and to help position the Met-20 side chain by making the appropriate hydrophobic interactions.

Why should the correct positioning of the Met-20 side chain matter? The recently proposed mechanism for N5 protonation of DHF [Figure 6 from Bystroff et al. (1990)] may give some insight into the question. According to this mechanism, an Asp-27-mediated proton transfer from fixed water-403 to O4 is followed by transfer of the proton from O4 to N5 via a second transiently bound water molecule. The latter would have to occupy a site that is otherwise occupied by Met-20. This water molecule would then be displaced by return of the Met-20 side chain to a position near N5 of DHF, effectively trapping the proton on the substrate in a hydrophobic environment. Thus, delocalization of the positive charge from N5 to C6 is encouraged, promoting hydride transfer from NADPH (Bystroff et al., 1990). This picture is consistent with the structure of recombinant human DHFR in a binary complex with 5-deazafolate. That structure shows side-chain atoms of Leu-22 (the functional equivalent of Met-20 in *E. coli* DHFR) moving by as much as 2.0 Å to make hydrophobic contact with C5 of 5-deazafolate when the latter inhibitor is substituted for folate (Davies et al., 1990).

ACKNOWLEDGMENTS

We thank Lynn Ten Eyck for assistance with the crystallographic least-squares refinement, Steve Dempsey and Jerry Greenberg for assistance with computer graphics, the San Diego Supercomputer Center for a generous grant allowing the crystallographic model building and structure refinement, and John Hirai for providing us with his unpublished $K_{m(NADPH)}$ vs pH profile for wt DHFR, as well as assistance with the HPLC purification of NADPH.

REFERENCES

Adams, J., Johnson, K., Matthews, R., & Benkovic, S. J. (1989) *Biochemistry 28*, 6611–6618.

Anderson, D. (1987) Ph.D. Thesis, University of California, San Diego, La Jolla, CA.

Andrews, J., Fierke, C. A., Birdsall, B., Ostler, G., Feeney, J., Roberts, G. C. K., & Bekovic, S. J. (1989) *Biochemistry 28*, 5743–5750.

Baccanari, D., Phillips, A., Smith, S., Sinski, D., & Burchall, J. (1975) *Biochemistry 14*, 5267–5273.

Baccanari, D. P., Stone, D., & Kuyper, L. (1981) *J. Biol. Chem. 256*, 1738–1747.

Beard, W. A., Appleman, J. R., Huang, S., Delcamp, T. J., Freisheim, J. H., & Blakley, R. L. (1991) *Biochemistry 30*, 1432–1440.

Benkovic, S. J., Fierke, C. A., & Naylor, A. M. (1988) *Science 239*, 1105–1110.

Birdsall, B., Andrews, J., Ostler, G., Tendler, S. J. B., Feeney, J., Roberts, G. C. K., Davies, R. W., & Cheung, H. T. A. (1989) *Biochemistry 28*, 1353–1362.

Blakley, R. L. (1960) *Nature (London) 40*, 1684–1685.

Blakley, R. L. (1984) in *Folates and Pterins, Vol. 1, Chemistry and Biochemistry of Folates* (Blakley, R. L., & Benkovic, S. J., Eds.) pp 191–253, John Wiley & Sons, New York.

Bolin, J. T., Filman, D. J., Matthews, D. A., Hamlin, R. C., & Kraut, J. (1982) *J. Biol. Chem. 257*, 13650–13662.

Bystroff, C., & Kraut, J. (1991) *Biochemistry 30*, 2227–2239.

Bystroff, C., Oatley, S. J., & Kraut, J. (1990) *Biochemistry 29*, 3263–3277.

Cayley, P. J., Dunn, S. M. J., & King, R. W. (1981) *Biochemistry 20*, 874–879.

Chen, J.-T., Taira, K., Tu, C.-P. D., & Benkovic, S. J. (1987) *Biochemistry 26*, 4093–4100.

Cleland, W. W. (1977) *Adv. Enzymol. Relat. Areas Mol. Biol. 45*, 273–387.

Cook, P. F., Kenyon, G. L., & Cleland, W. W. (1981) *Biochemistry 20*, 1204–1210.

Cork, C., Fehr, D., Hamlin, R., Vernon, W., Xuong, N.-H., & Perez-Mendez, V. (1973) *J. Appl. Crystallogr. 7*, 319–323.

Davies, J. F., Delcamp, T. J., Prendergast, N. J., Ashford, V. A., Freisheim, J. H., & Kraut, J. (199) *Biochemistry 29*, 9467–9479.

Ellis, K. J., & Morrison, J. F. (1982) *Methods Enzymol. 87*, 405–426.

Fersht, A. (1985) in *Enzyme Structure and Mechanism*, 2nd ed., pp 92–103, W. H. Freeman and Co., New York.

Fierke, C. A., & Benkovic, S. J. (1989) *Biochemistry 28*, 478–486.

Fierke, C. A., Johnson, K. A., & Benkovic, S. J. (1987) *Biochemistry 26*, 4085–4092.

Filman, D. J., Bolin, J. T., Matthews, D. A., & Kraut, J. (1982) *J. Biol. Chem. 257*, 13663–13672.

Gornall, A. G., Bardawill, C. J., & David, M. M. (1949) *J. Biol. Chem. 177*, 751–766.

Hillcoat, B. L., Nixon, P. F., & Blakley, R. L. (1967) *Anal. Biochem. 21*, 178–189.

Howell, E. E., Villafranca, J. E., Warren, M. S., Oatley, S. J., & Kraut, J. (1986) *Science 231*, 1123–1128.

Howell, E. E., Warren, M. S., Booth, C. L. J., Villafranca, J. E., & Kraut, J. (1987) *Biochemistry 26*, 8591–8598.

Howell, E. E., Foster, P. G., & Foster, L. M. (1988) *J. Bacteriol. 170*, 3040–3045.

Howell, E. E., Booth, C., Farnum, M., Kraut, J., & Warren, M. S. (1990) *Biochemistry 29*, 8561–8569.

Huang, S., Delcamp, T. J., Tan, X. H., Smith, P. L., Prendergast, N. J., & Freisheim, J. H. (1989) *Biochemistry 28*, 471–478.

Johnson, S. L., & Tuazon, P. T. (1977) *Biochemistry 16*, 1175–1183.

Jones, T. A. (1978) *J. Appl. Crystallogr. 11*, 268–272.
Kaufman, B. T., & Gardiner, R. C. (1966) *J. Biol. Chem. 241*, 1319–1328.
Lagosky, P. A., Taylor, G. R., & Haynes, R. H. (1987) *Nucleic Acids Res. 15*, 10355–10371.
Leatherbarrow, R. J. (1987) ENZFITTER: A Non-Linear Regression Data Analysis Program for the IBM PC, Elsevier-BIOSOFT, London.
Maharaj, G., Selinsky, B. S., Appleman, J. R., Perlman, M., London R. E., & Blakley, R. L. (1990) *Biochemistry 29*, 4554–4560.
Matthews, D. A., Alden, R. A., Bolin, J. T., Freer, S. T., Hamlin, R., Xuong, N.-H., Kraut, J., Poe, M., Williams, M., & Hoogsteen, K. (1977) *Science 197*, 452–455.
Matthews, D. A., Alden, R. A., Bolin, D. J., Filman, J. D., Freer, S. T., Hamlin, R., Hol, W. G. J., Kisliuk, R. L., Pastore, E. J., Plante, L. T., Xuong, N.-H., & Kraut, J. (1978) *J. Biol. Chem. 253*, 6946–6954.
Matthews, D. A., Alden, R. A., Freer, S. T., Xuong, N.-H., & Kraut, J. (1979) *J. Biol. Chem. 254*, 4144–4151.
Matthews, D. A., Bolin, J. T., Burridge, J. M., Filman, D. J., Volz, K. W., Kaufman, B. T., Beddell, C. R., Champness, J. N., Stammers, D. K., & Kraut, J. (1985a) *J. Biol. Chem. 260*, 381–391.
Matthews, D. A., Bolin, J. T., Burridge, J. M., Filman, D. J., Volz, K. W., & Kraut, J. (1985b) *J. Biol. Chem. 260*, 392–399.
Maniatis, T., Fritsch, E. F., & Sambrook, J. (1982) *Molecular Cloning, A Laboratory Manual*, p 440, Cold Spring Harbor Laboratory, Cold Spring Harbor, NY.
Mayer, R. J., Chen, J.-T., Taira, K., Fierke, C. A., & Benkovic, S. J. (1986) *Proc. Natl. Acad. Sci. U.S.A. 83*, 7718–7720.
Morrison, J. F., & Stone, S. R. (1988) *Biochemistry 27*, 5499–5506.
Murphy, D. J., & Benkovic, S. J. (1989) *Biochemistry 28*, 3025–3031.
Oefner, C., D'Arcy, A., & Winkler, F. K. (1988) *Eur. J. Biochem. 174*, 377–385.
Oppenheimer, N. J., & Kaplan, N. O. (1974) *Biochemistry 13*, 4675–4685.
Orr, G. A., & Blanchard, J. S. (1984) *Anal. Biochem. 142*, 232–234.
Pattishall, K. H., Burchall, J. J., & Harvey, R. J. (1976) *J. Biol. Chem. 251*, 7011–7020.
Penner, M. H., & Frieden, C. (1985) *J. Biol. Chem. 260*, 5366–5369.
Poe, M. (1977) *J. Biol. Chem. 252*, 3724–3728.
Prendergast, N. J., Appleman, J. R., Delcamp, T. J., Blakley, R. L., & Freisheim, J. H. (1989) *Biochemistry 28*, 4645–4650.
Sanger, F., Nicklen, S., & Coulson, A. R. (1977) *Proc. Natl. Acad. Sci. U.S.A. 74*, 5463–5467.
Sanger, F., Coulson, A. R., Barrell, B. G., Smith, A. J. H., & Roe, B. A. (1980) *J. Mol. Biol. 143*, 161–178.
Schweitzer, B. I., Srimatkandada, S., Gritsman, H., Sheridan, R., Venkataraghavan, R., & Bertino, J. R. (1989) *J. Biol. Chem. 264*, 20786–20795.
Spears, G., Snyed, J. G. T., & Loten, E. G. (1971) *Biochem. J. 125*, 1149–1151.
Srinivasan, R., & Fisher, H. F. (1985) *J. Am. Chem. Soc. 107*, 4301–4305.
Stammers, D. K., Champness, J. N., Beddell, C. R., Dann, J. G., Eliopoulos, E., Geddes, A. J., Ogg, D., & North, A. C. T. (1987) *FEBS Lett. 218*, 178–184.
Stone, S. R., & Morrison, J. F. (1983) *Biochim. Biophys. Acta 745*, 247–258.
Stone, S. R., & Morrison, J. F. (1984) *Biochemistry 23*, 2753–2758.
Stone, S. R., & Morrison, J. F. (1986) *Biochim. Biophys. Acta 869*, 275–285.
Stone, S. R., & Morrison, J. F. (1988) *Biochemistry 27*, 5493–5499.
Taira, K., & Benkovic, S. J. (1988) *J. Med. Chem. 31*, 129–137.
Tartof, K. D., & Hobbs, C. A. (1987) *Bethesda Research Laboratories Focus 9*, 12.
Thillet, J., Absil, J., Stone, S. R., & Pictet, R. (1988) *J. Biol. Chem. 263*, 12500–12508.
Tronrud, D. E., Ten Eyck, L. F., & Matthews, B. W. (1987) *Acta Crystallogr. A43*, 489–501.
Tsay, J.-T., Appleman, J. R., Beard, W. A., Prendergast, N. J., Delcamp, T. J., Freisheim, J. H., & Blakley, R. L. (1990) *Biochemistry 29*, 6428–6436.
Villafranca, J. E., Howell, E. E., Voet, D. H., Strobel, M. S., Ogden, R. C., Abelson, J. N. & Kraut, J. (1983) *Science 222*, 782–788.
Volz, K. W., Matthews, D. A., Alden, R. A., Freer, S. T., Hansch, C., Kaufman, B. T., & Kraut, J. (1982) *J. Biol. Chem. 257*, 2528–2536.
Williams, J. W., Morrison, J. F., & Duggleby, R. G. (1979) *Biochemistry 18*, 2567–2573.
Xuong, N.-H., Nielson, C. P., Hamlin, R., & Anderson, D. H. (1985) *J. Appl. Crystallogr. 18*, 342–350.